Kidney International, Vol. 17 (1980), pp. 771–787

Proteinuria induced by sodium maleate in rats: Effects on ultrastructure and protein handling in renal proximal tubule

ERIK ILSØ CHRISTENSEN and ARVID B. MAUNSBACH

Department of Cell Biology, Institute of Anatomy, University of Aarhus, Aarhus, Denmark

Proteinuria induced by sodium maleate in rats: Effects on ultrastructure and protein handling in renal proximal tubule. We studied the effects of sodium maleate on renal handling of protein in rats injected i.v. with sodium maleate. We used lysozyme (mol wt, 14,400 daltons) labeled with iodine 125 as a tracer. We studied the protein reabsorption and transport in the renal proximal tubule cells, electron microscope autoradiography, and we followed the lysosomal digestion of lysozyme in renal cortical slices. Maleate decreased glomerular filtration and tubular reabsorption of lysozyme but caused an increased urinary excretion. The digestion of reabsorbed lysozyme was considerably reduced in renal cortical slices, and autoradiography revealed that the transport of protein from endocytic vacuoles to lysosomes in proximal tubule cells was partially inhibited. After maleate treatment, endocytic vacuoles rapidly accumulated in the apical cytoplasm but apical tubules disappeared, indicating an altered recycling of membrane. An ultrastructural morphometric analysis substantiated and extended the qualitative observations and provided quantitative estimates of volumes and surface areas for endocytic vacuoles, apical tubules, lysosomes, and microvilli in control and experimental animals. The tubule cells were ultrastructurally normal 48 hours after the injection of maleate. *Conclusion.* Sodium maleate causes proteinuria due to a decreased tubular reabsorption of protein, and it demonstrates a decreased transport of protein from endocytic vacuoles to lysosomes in proximal tubule cells and a subsequent low tubular protein catabolism.

Protéinurie déterminée par let maleate de sodium chez le rat: Effets sur l'ultrastructure du tube proximal et sur le comportement des protéines. Les effets du maléate de sodium sur le comportement rénal des protéines ont été étudiés chez des rats ayant reçu du maléate de sodium par voie intraveineuse. Le lysosyme (PM 14.400 daltons) marqué par iodine 125 a été utilisé comme traceur. La réabsorption et le transport de protéines dans les cellules tubulaires rénales proximales ont été suivis par autoradiographie en microscopie électronique et par l'étude, dans des tranches de cortex, de la digestion lysosomale du lysosyme. Le maléate a diminué la filtration glomérulaire et la réabsorption tubulaire du lysosyme mais en a augmenté l'excrétion urinaire. La digestion du lysosyme réabsorbé a été considérablement diminuée dans les tranches de cortex et l'autoradiographie a montré que le transport des protéines des vacuoles d'endocytose aux lysosomes des cellules tubulaires proximales était partiellement inhibé. Après un traitement par le maléate des vacuoles d'endocytose se sont rapidement accumulées dans le cytoplasme apical alors que les tubules apicaux disparaissaient, ce qui indique une modification du renouvellement de la membrane. Une analyse morphométrique ultrastructurale a étayé les observations qualitatives et fourni des évaluations quantitatives du volume et/ou de la surface des vacuoles d'endocytose, des tubules apicaux, des lysosomes et des microvillosités chez les animaux témois et expérimentaux. Les cellules tubulaires étaient normales en ultrastructure 48 heures après l'injection de maléate. *Conclusion.* Le maléate de sodium détermine une protéinurie du fait de la réabsorption tubulaire des protéines et font la preuve de la diminution du transport des protéines des vacuoles d'endocytose aux lysosomes des cellules tubulaires proximales et d'un faible catabolisme protéinique.

In experimental animals, the injection of sodium maleate produces a renal syndrome consisting of increased diuresis, phosphaturia, aminoaciduria, and glucosuria [1–3]. This syndrome, which in some respects resembles the De Toni-Debré Fanconi syndrome [2], is probably due to interference with metabolic processes in the tubule cells. Thus, sodium maleate has been shown to inhibit the oxidation of different CoA-dependent substrates [4] and has also been demonstrated to decrease the activity of renal Na-K-ATPase and renal cortical concentration of ATP [5].

In addition to functional and metabolic changes, sodium maleate produces extensive ultrastructural changes in the kidney, especially in the proximal tubule cells, which show increased cytoplasmic vacuolization and enhanced electron density in the mitochondrial matrix [6–8].

Because sodium maleate also produces tubular proteinuria in experimental animals [9–12], we were interested in studying the concomitant structural and functional effects of sodium maleate on proximal tubular uptake, transport, and digestion of a low-molecular-weight protein, with the aim of obtaining additional information about how these processes related to tubule cell ultrastructure and to

Received for publication July 10, 1979
and in revised form November 4, 1979

0085-2538/80/0017-0771 $03.40

determine the mechanism of proteinuria in this experimental model. For the tracer protein, we used lysozyme, which we have previously used to study renal handling of protein in the normal kidney [13].

The combined results of this study reveal that the i.v. injection of sodium maleate reduces the endocytic uptake by the proximal tubule cells of low-molecular-weight protein and decreases the transport of protein into lysosomes, thus reducing the catabolism of reabsorbed protein.

Methods

Animals. Adult male Wistar rats 2.5 to 5.0 months of age were used in all experiments.

Iodination of lysozyme. Lysozyme obtained from egg white (Grade I, Sigma Chemical Company) was iodinated with either iodine 131 or 125 according to the iodine monochloride method of McFarlane [14] as modified by Izzo et al [15]. The molar ratio of iodine monochloride to lysozyme was 1:1. Free iodine was removed by passage through a column of Sephadex G-25 medium and subsequent dialysis of the effluent against 0.9% sodium chloride. The iodination efficiency using iodine 131 was 37.9%. The specific activity in the final solution was 0.26 mCi/mg of lysozyme, and free iodine represented 1.9% of total radioactivity determined as TCA (trichloroacetic acid)-soluble radioactivity. The enzymatic activity of lysozyme per milligram of protein, as determined after iodination by the method of Litwack [16], was 92% of the activity of noniodinated lysozyme. The protein concentration was determined by the method of Lowry et al [17]. The average iodination efficiency in iodinations with iodine 125 was 71%, the average specific activity was 0.42 mCi/mg of lysozyme, and free iodine never represented more than 3% of the total activity in the final solutions. The enzymatic activity of lysozyme was never lower than 91%, as compared to noniodinated lysozyme.

Digestion of ^{125}I-lysozyme in renal cortical slices. Maleic acid, 400 mg/kg body wt, was given i.v. to rats as a solution, which contained 100 mg/ml of water and was brought to pH 7.4 with sodium hydroxide. Five minutes later, the animals were injected i.v. with 0.2 to 0.5 ml of ^{125}I-lysozyme. Control rats were given the same volume (4 ml/kg body wt) of 0.9% sodium chloride prior to the injection of lysozyme. After the injection of labeled protein (15 or 60 min), slices were removed from the renal cortex with a Stadie-Riggs-type microtome, as described by Maude [18] while the kidneys were perfused retrograde through the aorta with a bicarbonate saline solution [18] at 4° C (pH, 7.4). The slices were incubated in vitro for up to 2 hours, as previously described [13], in the same solution as used for the perfusion. The digestion of protein was determined as the TCA-soluble radioactivity appearing in incubation medium and remaining in the tissue slices, expressed in percent of total radioactivity. Radioactivity was measured in a gamma counter (Selektronik, Copenhagen).

In other experiments, cortical slices from rats injected 15 or 60 min previously with the labeled lysozyme only were incubated in vials containing 2 ml of the bicarbonate-saline solution as above, but with the addition of 2.5 mg of sodium maleate per milliliter at a pH of 7.4.

GFR and glomerular filtration of lysozyme. The GFR was determined from the inulin clearance. Animals were anesthetized with Inactin® (100 mg/kg body wt), placed on a heated operating table where the body temperature was maintained at 37° C, and tracheotomized. The jugular veins were cannulated for single injections and infusion of inulin and ^{131}I-lysozyme. The carotid artery was cannulated for blood sampling and monitoring of blood pressure, and one ureter was cannulated for urine sampling. Immediately after the injection of sodium maleate, there was a pronounced decrease in the blood pressure, which, however, again reached normal values within 2 or 3 min. The rats received a bolus injection of 20 μCi of ^{3}H-inulin in 0.5 ml of lactate buffer (pH, 7.2), followed by a constant infusion of a solution containing 10 μCi of ^{3}H-inulin per milliliter of lactate buffer, at a rate of 1.9 ml/hr.

The GFR was first determined for 1 hour during three consecutive 20-min periods. One of the following solutions was then injected into the femoral vein in the same volumes (4 ml/kg body wt): *(1)* sodium maleate (100 mg/ml) at a dose corresponding to 400 mg sodium maleate per kilogram of body weight, *(2)* 6.0% sodium chloride, which has the same osmolality as 100 mg/ml neutralized sodium maleate, and *(3)* 0.9% sodium chloride. Five minutes later, the animals received a bolus injection of 8.3 μCi of ^{131}I-lysozyme in 0.2 ml of lactate buffer followed by a constant infusion (rate, 1.9 ml/hr) for 15 min of a lactate buffer solution containing 10 μCi of ^{3}H-inulin and 12.5 μCi of ^{131}I-lysozyme per milliliter. At the end of the infusion period, the urine was collected, a blood sample was taken, and the kidneys were perfused retrograde through the aorta with a Ringer solution at 4° C. ^{131}I-lysozyme in urine, plasma, and in excised kidneys was counted in a gamma counter, and ^{3}H-inulin was counted in a

liquid scintillation counter (Beckman LS-133). The amount of lysozyme filtered was expressed as the sum of the lysozyme reabsorbed and retained in the kidneys and the amount excreted in the urine. The fractional clearance of lysozyme (expressed in percent) was determined as 100 × clearance of lysozyme/GFR.

Electron microscope procedures. For the morphometric studies, the kidneys of rats injected with either sodium meleate or 6.0% sodium chloride were fixed by retrograde perfusion through the aorta after 15 or 60 min; for quantitative studies rats were fixed after postinjection periods of up to 7 days. The fixative consisted of 1% glutaraldehyde in a Tyrode's solution, modified with respect to the sodium chloride concentration [19] (sodium chloride, 6 g/liter, 75% of the normal amount of socium chloride). The tissue was then further fixed by immersion in 3% glutaraldehyde in 0.1 M sodium cacodylate buffer (pH, 7.2), postfixed in 1% osmium tetroxide in veronal acetate buffer (pH, 7.2), dehydrated in alcohol, and embedded in Epon 812. Semithin (0.5 to 1 μm) or ultrathin sections were cut on a LKB Ultrotome III. The ultrathin sections were stained with uranyl acetate and lead citrate and studied either in a Jeol 100 B or 100 C electron microscope.

Morphometric analysis. For morphometric study, one cross-sectioned tubule (longest diameter/shortest diameter, < 1.5) from each animal was photographed at a magnification of ×6600, using only the lower left quadrant of the tubules as seen in the electron microscope. All tubular cross-sections were derived from the convoluted part of the proximal tubule. The area occupied by the proximal tubule cells minus the brush border was used as reference area for all morphometric determinations. There were five animals in each of four groups, that is, animals fixed by perfusion for either 15 or 60 min after i.v. injection of either sodium maleate or 6.0% chloride as described above. Following photographic enlargement to a final magnification of about ×20,000, the exact magnifications were determined by using a carbon replica (2160 lines/mm). A coherent lattice square test system was used for point counting and intersection counting [20]. The distance between the heavy lines and the fine lines was 20 mm and 4 mm, respectively, corresponding to about 1 μm and 0.2 μm.

The following parameters were determined by point counting and intersection counting [20]: The volume density (V_V), expressed in percent (100 × $\mu m^3/\mu m^3$, by point counting and the surface density (S_V), expressed in square micrometer per square micrometer, by intersection counting of the lysosomes, endocytic vacuoles, and the volume density only of the apical tubules. The surface density was calculated by the formula $S_V = 2N/L_T$, in which N is the number of intersections and L_T is the length of test line [20]. To reduce the Holmes effect (effect of section thickness) and the effects of difficulties in distinguishing profiles in the section [21], we determined the surface density of the brush border and the apical tubules by measuring the diameter and by counting the profiles of apical tubules and microvilli using the formula $S_V = 2N_A \times \pi \times d$, in which N_A is the number of profiles per test area (test area: corresponding proximal tubule cells minus the brush border) and d is the diameter of the apical tubules or the microvilli. The profiles were counted in a lattice square test system [22] with a distance between lines of 20 mm. Profiles were counted in every fourth square. The diameter (d) measured on profiles of 414 apical tubules and 317 microvilli selected at random, as above, was 0.0842 μm and 0.0919 μm, respectively. There were no differences in the diameter of the apical tubules or the microvilli between the different groups, that is, sodium-maleate-treated animals vs. control animals. Assuming that the lysosomes are spherical particles, the mean diameter of the lysosomal profiles (D) was calculated from the following formula: $D = 6V_V/S_V$ [23].

Volume densities (V_V) and surface densities (S_V) were converted to micrometer^3 and micrometer^2 per millimeter of tubule length by multiplying the total area (μm^2) of the cross-sectioned tubule with 10^3. This conversion was carried out because the cell area per cross section tubule was reduced in sodium-maleate-treated rats as compared with controls. The diameter of the proximal tubules was measured on semithick sections stained with toluidine blue by light microscopy. One section from each of five animals from each of the above mentioned four groups was studied at a magnification of ×600. The shortest diameters, outer and inner, were measured in all tubules that were approximately cross-sectioned, that is, largest diameter/shortest diameter ratio less than 1.5. The inner luminal diameter was measured from the base of the brush border, and the height of the proximal tubule cells was calculated as half the difference between the peritubular diameter and the luminal diameter.

Electron microscope histochemistry. For histochemical studies, kidneys from rats injected with sodium maleate were fixed by perfusion with 1% glutaraldehyde in 0.1 M cacodylate buffer, (pH, 7.2)

and postfixed for 2 hours in 3% glutaraldehyde in the same buffer. Acid phosphatase activity was demonstrated by incubation of the tissue in the Gomori medium as modified by Barka and Anderson [24]. The incubations were carried out at 37° C for 10 min at a pH of 5.4. The tissue was then postfixed in 1% osmium tetroxide and further treated as described above. Controls were incubated in the absence of substrate or in the presence of 10 mM sodium fluoride.

Electron microscope autoradiography. Rats were injected first with either 6.0% sodium maleate or 0.9% sodium chloride and five min later with 0.5 ml ^{125}I-lysozyme. After either 15 or 60 min, the kidneys (two rats in each group at each time) were fixed by perfusion and the tissue samples were prepared for electron microscopy as described above.

Thin sections were stained with uranyl acetate and lead citrate and covered with Ilford L4 emulsion by the wire-loop method as described by Maunsbach [25]. The grids were exposed from 14 days to 3 months, developed in Kodak D19 developer for 90 sec and fixed for 2 min in 20% sodium thiosulphate.

The grain distribution was determined over two cross-sectioned proximal tubules from each animal. The tubules were photographed at a magnification of ×5000, and the micrographs were enlarged 2.3 times. The autoradiographic background, which never exceeded 0.005 grains/μm^2, was determined by counting grains over Epon from the same section or over the formvar film adjacent to the section. Grains were counted over the following regions: endocytic vacuoles; E-cytoplasm (the cytoplasm within 0.5 μm from endocytic vacuoles, exclusive of other cell organelles over which grains were counted); lysosomes; L-cytoplasm (the cytoplasm within 0.5 μm from the lysosomal membrane); brush border; cytoplasm (the remaining cell area including the cell nucleus); and the basement membrane. This was expressed as the percent of the total number of grains.

Results

Ultrastructure of proximal tubule cells after sodium maleate injection. As compared with controls, there was a reduction in the height of the proximal tubule cells 20 min after injection of sodium maleate (Figs. 1 and 2), and there was an increase in the number of small endocytic vacuoles (Fig. 2). After 1 hour these changes were even more pronounced, and the accumulation of apical vacuoles was quite prominent. Many mitochondria had their long axis almost parallel to the basement membrane (Fig. 3). Most of the apical tubules had disappeared (Figs. 4 and 5), and the coat on the inside of membranes of the endocytic vacuoles in the maleate-treated animals appeared thinner than it did in controls (Figs. 4 and 5). Some lysosomes, identified by means of the cytochemical reaction for acid phosphatase (Fig. 6), appeared enlarged and more electron-translucent (Fig. 3) than they did in controls. The apical vacuoles did not show acid phosphatase activity. The ultrastructure of the cell membrane, including cell junctions and the smooth endoplasmic reticulum, appeared qualitatively unaltered. The alterations induced by sodium maleate were observed throughout the convoluted part of the proximal tubule.

After 4 hours (Fig. 7), numerous small vacuoles occupied the upper half of the proximal tubule cells. Most mitochondria were markedly condensed, but some mitochondria were swollen, and the granular endoplasmic reticulum was distended. There was a much decreased frequency of polyribosomes, and instead single ribosomes were dispersed throughout the cytoplasm (Fig. 7), including the basal parts of the microvilli (inset to Fig. 7).

After 24 hours, most tubules appeared normal (Fig. 8) except for an increased autophagocytosis and a few swollen mitochondria (Fig. 8). In 5 to 10% of the proximal tubules, however, most cells appeared necrotic. In these tubules, the basement membrane was in places denuded, and viable cells extended along the basement membrane, partially covering the denuded areas (Fig. 9). After 48 hours, all tubules appeared normal.

Morphometric analysis of proximal tubule cells. The volume density of the small endocytic vacuoles increased in sodium-maleate-treated animals as compared with control animals, and there was also an increase from 20 to 60 min in the sodium-maleate-treated animals (Table 1). When calculated per millimeter of tubule length, there was in increase in the volume of small endocytic vacuoles from 20 to 60 min in sodium-maleate-treated rats, and the volume of the vacuoles was also larger in 60-min sodium-maleate-treated rats as compared with the 60-min controls (Table 1).

The surface density of small endocytic vacuoles was also increased in sodium-maleate-treated animals (Table 2). The surface area per millimeter of tubule length of small endocytic vacuoles was significantly increased in 60-min sodium-maleate-treated rats as compared with 60-min controls. The surface density and the surface per millimeter of tubule length was also significantly increased when

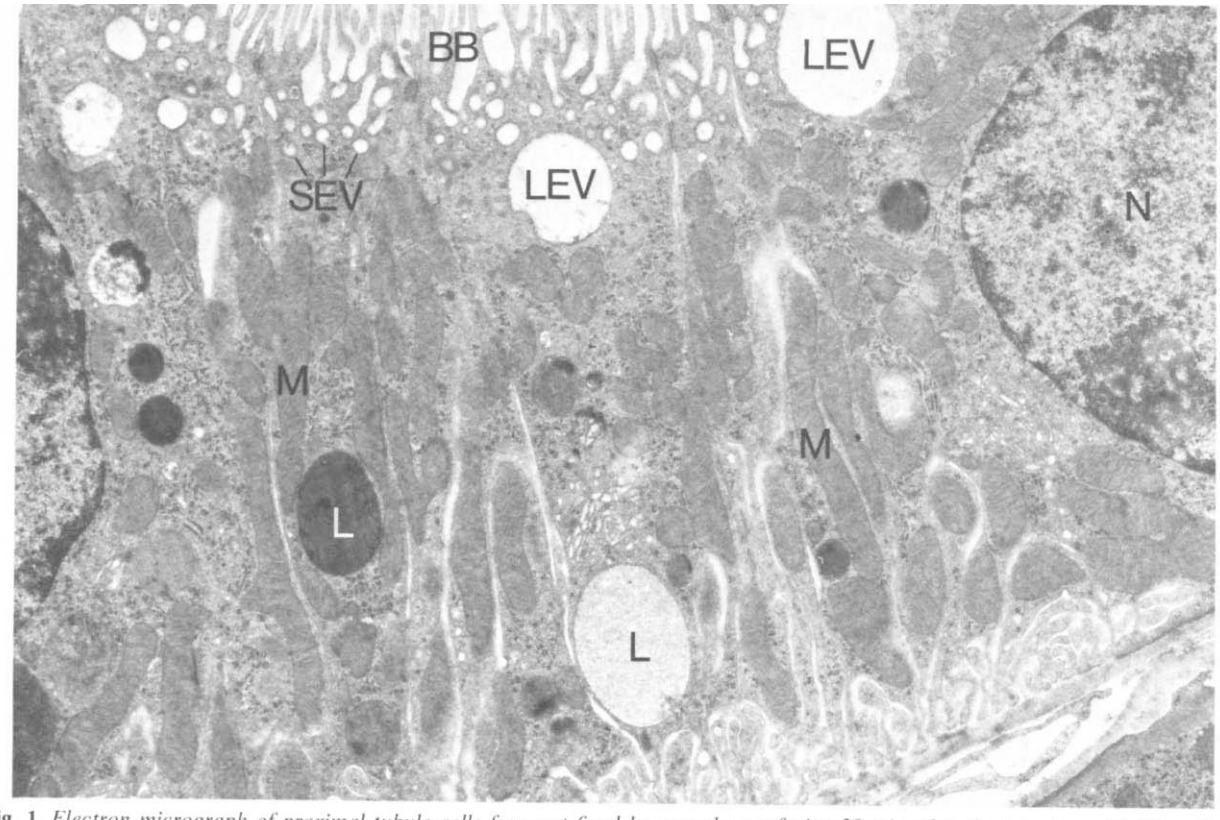

Fig. 1. *Electron micrograph of proximal tubule cells from rat fixed by vascular perfusion 20 min after the injection of 6.0% sodium chloride (control).* In the cytoplasm below the brush border (BB), there are small (SEV) and large endocytic vacuoles (LEV). L is lysosomes; N, nucleus; M, mitochondria. (×9500)

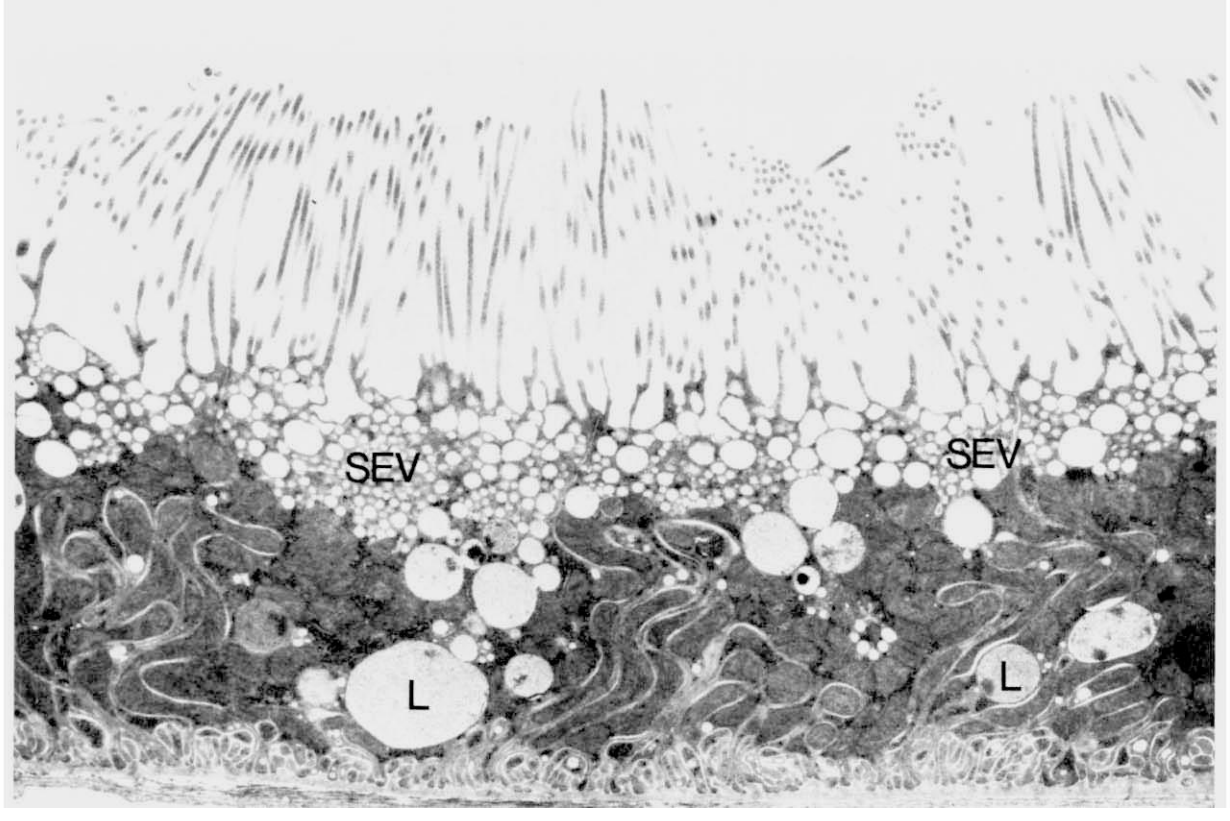

Fig. 2. *Electron micrograph of proximal tubule cells from rat fixed by vascular perfusion 20 min after the injection of sodium maleate.* There is a reduction of the cell height and an increased number of small endocytic vacuoles (SEV). The mitochondria (M) appear somewhat condensed. L is lysosomes. (×9500)

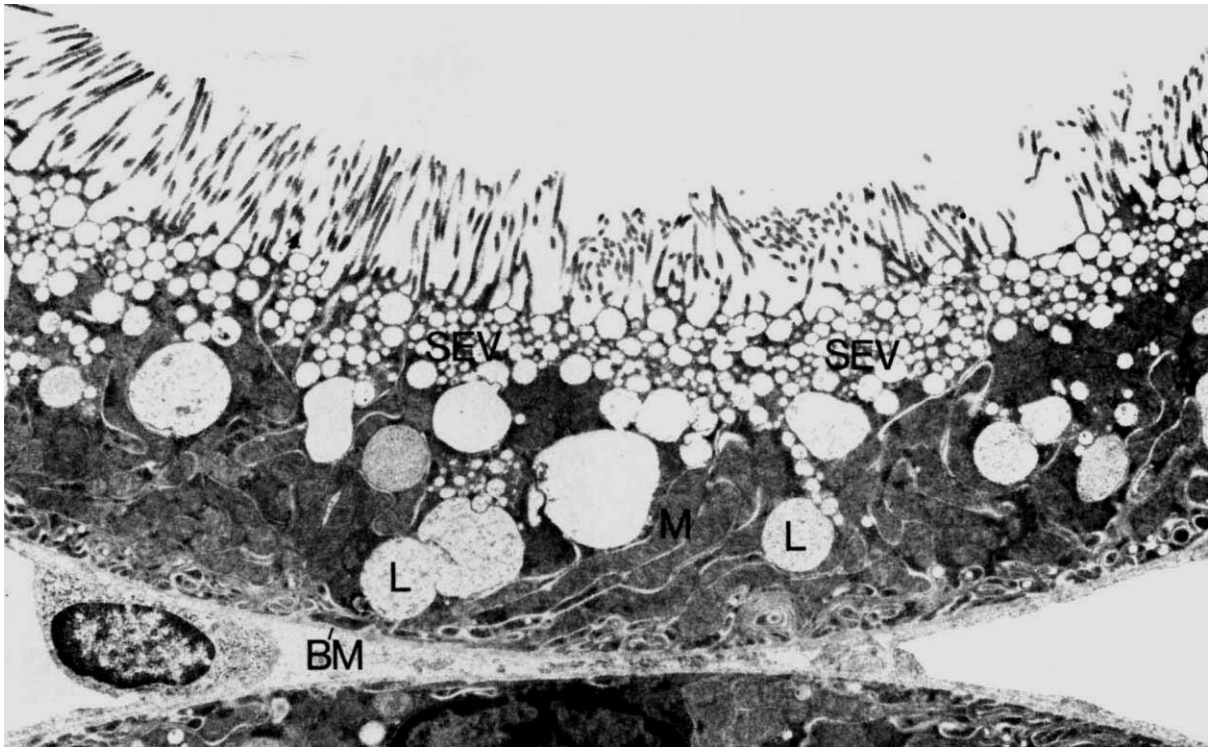

Fig. 3. *Electron micrograph of proximal tubule cells from rat fixed by vascular perfusion 60 min after injection of sodium maleate.* There is a large number of small endocytic vacuoles (SEV) in the apical part of the cells. The lysosomes are large and appear more electron-lucent than usual. At places, the long axis of the mitochondria (M) appears oriented more or less parallel to the basement membrane (BM). (×7300)

calculated for all endocytic vacuoles (Table 2). The small apical tubules in the proximal tubule cells largely disappeared after the maleate treatment (Tables 1 and 2; Figs. 4 and 5). The microvilli showed no changes in surface density or surface per millimeter of tubule length after sodium maleate treatment (Table 2).

There was a significant increase in the volume density of lysosomes in animals that received sodium maleate 60 min before fixation as compared with animals at 20 min and controls (Table 1). The absolute volume of lysosomes per millimeter of tubule length increased significantly between 20 and 60 min in sodium-maleate-treated animals. The average diameter of the lysosomal profiles was not different in controls and animals injected with sodium maleate 20 min before fixation. At 60 min after injection of sodium maleate, however, the diameter was increased about 75% when compared with 60-min control animals and 54% when compared with animals fixed 20 min after injection of sodium maleate (Table 3).

After sodium maleate injection, there was a 37% increase in the luminal diameter of the proximal tubules, and the height of the proximal tubule cells was reduced to 66% of controls (Table 3).

GFR and renal accumulation of lysozyme. After a single injection of sodium maleate, the GFR decreased during the first 20-min period to 52% of the control value, whereas the GFR did not change significantly in rats that received 0.9% sodium chloride or 6.0% sodium chloride (Table 4).

Urine flow (Table 4) increased about two times in the animals receiving 0.9% sodium chloride, 10 times in rats given 6.0% sodium chloride, and about 70 times in the animals given sodium maleate.

During maleate infusion, there was a decrease of the renal accumulation of lysozyme to 31% of that found in animals infused with 0.9% sodium chloride and at the same time a 73-fold increase in the urinary excretion of lysozyme (Table 4). The total glomerular filtration of lysozyme decreased, however, due to a decreased clearance of lysozyme and a decreased fractional clearance of lysozyme (Table 4).

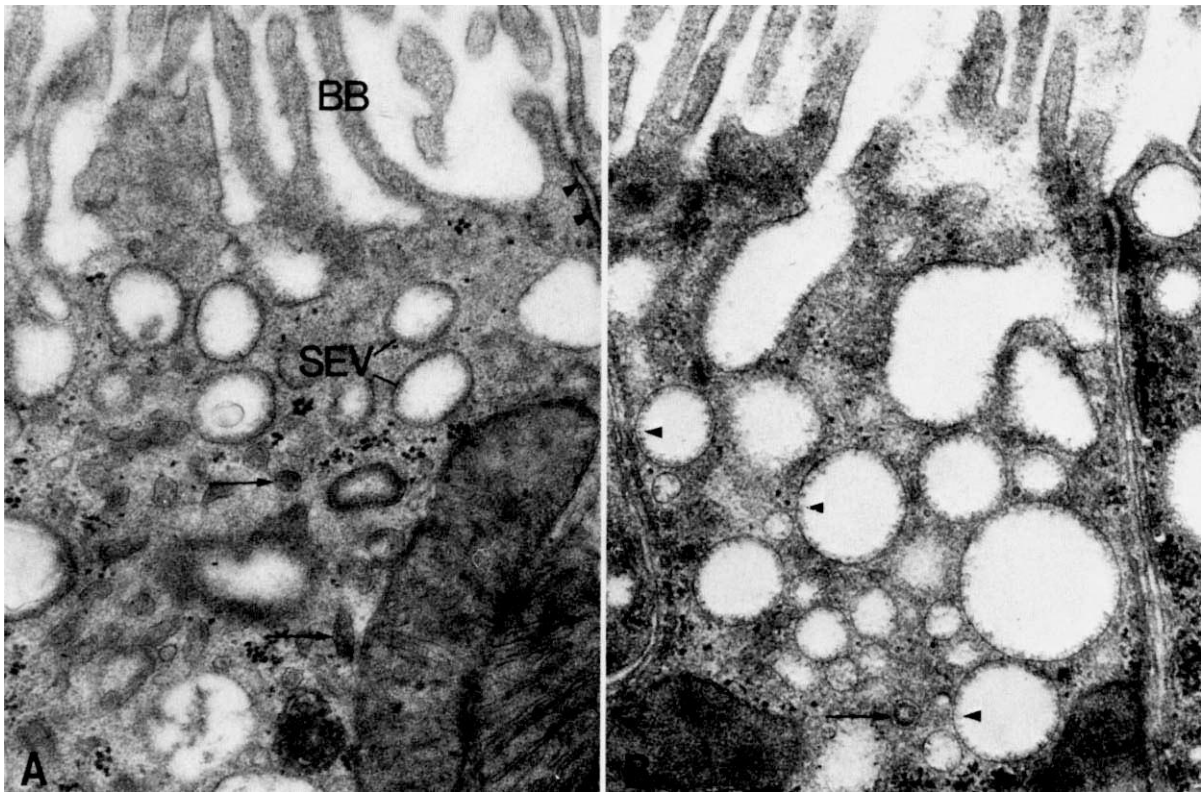

Fig. 4. *Electron micrograph of the apical part of a proximal tubule cell from rat fixed by vascular perfusion 1 hour after injection of 6.0% sodium chloride (control).* Small endocytic vacuoles (SEV) are seen below the brush border (BB), and the apical cytoplasm shows apical tubules (*arrows*) and a junctional complex (*arrowheads*). (×36,800)

Fig. 5. *Electron micrograph of the apical part of a proximal tubule cell from a rat prepared as in Fig. 3.* The membrane coat (*arrowheads*) in the endocytic vacuoles appears more fuzzy than it does in controls (compare with Fig. 4) and the apical tubules (*arrow*) are largely absent. Elements of the smooth endoplasmic reticulum follow the cell membranes and appear unchanged. (×36,800)

Intracellular transport of labeled lysozyme. Electron microscope autoradiography revealed evidence of a decreased transport of protein from endocytic vacuoles to the lysosomes in the proximal tubule cells in animals treated with sodium maleate as compared with controls (compare Figs. 10 and 12 to Figs. 11 and 13). Fifteen minutes after injection of labeled lysozyme, the accumulation in the lysosomes was 6.3% in maleate-treated rats as compared with 41.6% and 47.3% in controls given 0.9% and 6.0% sodium chloride, respectively (Table 5). After 1 hour, corresponding figures were 7.5%, 81.0%, and 70.4% (Table 5). In control rats, there was a decrease in the concentration of grains over the endocytic vacuoles between 15 and 60 min, but such a decrease was not seen in the sodium-maleate-treated rats (Table 5).

Digestion of protein in renal cortical slices. The digestion of protein was much decreased in renal slices from sodium-maleate-treated rats as compared with controls. After 120 min of incubation of slices removed 15 min after injection of lysozyme the digestion decreased from 33.3% to 6.5% (Fig. 14); and in slices removed after 60 min, from 45.1% to 13.0% (Fig. 15). Thus, the demonstrated decreases in protein digestion were 80 and 71%, respectively. The initial rate of digestion was lower in slices removed after 15 min (Fig. 14) than it was in slices removed after 60 min (Fig. 15).

In slices from nontreated animals injected with labeled lysozyme and incubated for 120 min in the presence of sodium maleate (2.5 mg/ml), there was a 58% decrease in the digestion of lysozyme in slices removed after 15 min and a 35% decrease in slices removed after 60 min. In the latter slices, there was initially only a small inhibitory effect of sodium maleate (Fig. 16).

Discussion

The present study revealed that i.v. injection of sodium maleate decreased the reabsorption of lysozyme by the proximal tubule cells, reduced the

Fig. 6. *Electron micrograph of proximal tubule cells from rat fixed by vascular perfusion 60 min after the injection of sodium maleate.* The tissue has been incubated for the demonstration of acid phosphatase. The large irregular lysosomes (L) show reaction for acid phosphatase. (×12,000)

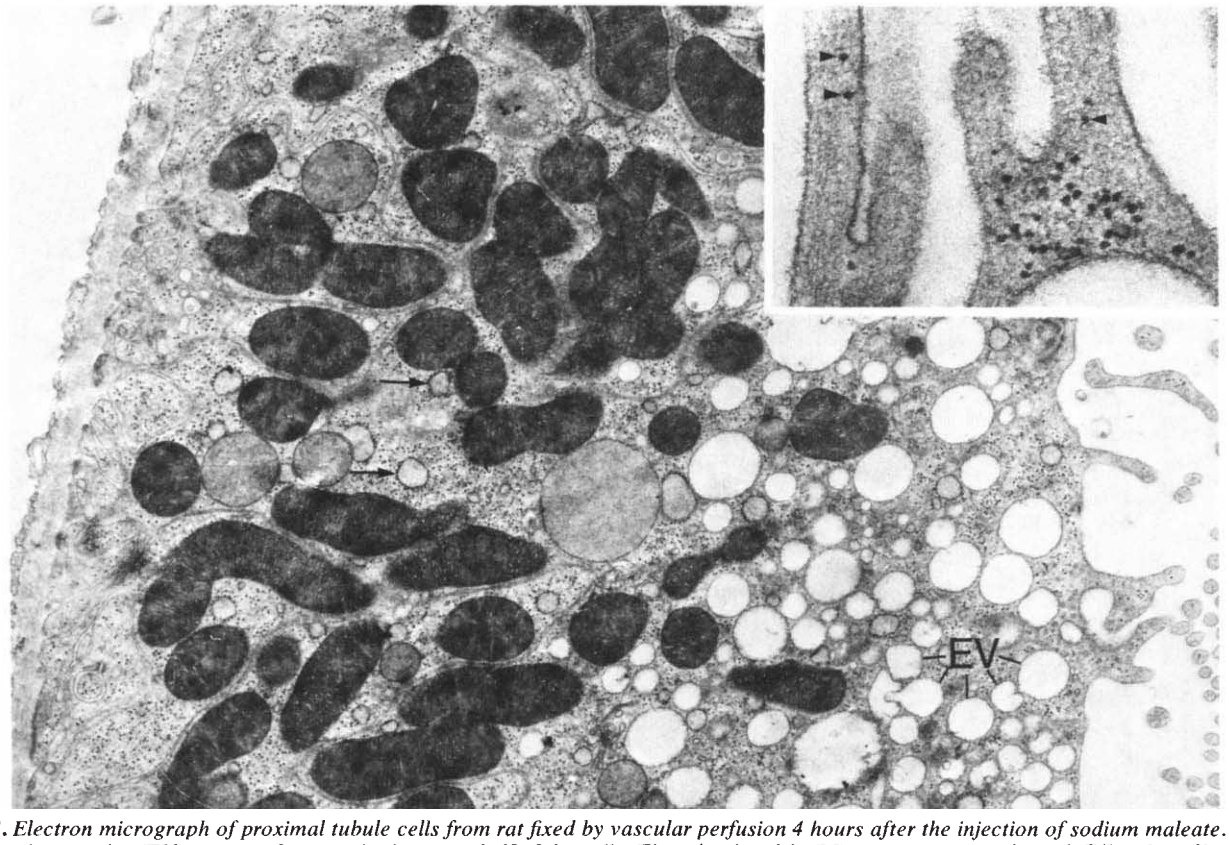

Fig. 7. *Electron micrograph of proximal tubule cells from rat fixed by vascular perfusion 4 hours after the injection of sodium maleate.* Endocytic vacuoles (EV) are very frequent in the upper half of the cells. The mitochondria (M) appear very condensed. Dilated profiles of granular endoplasmic reticulum (*arrows*) are found in the cytoplasm, and single ribosomes are seen scattered all over in the cytoplasm and even found in the microvilli (*arrowheads on inset*). (×15,200; inset, ×87,000)

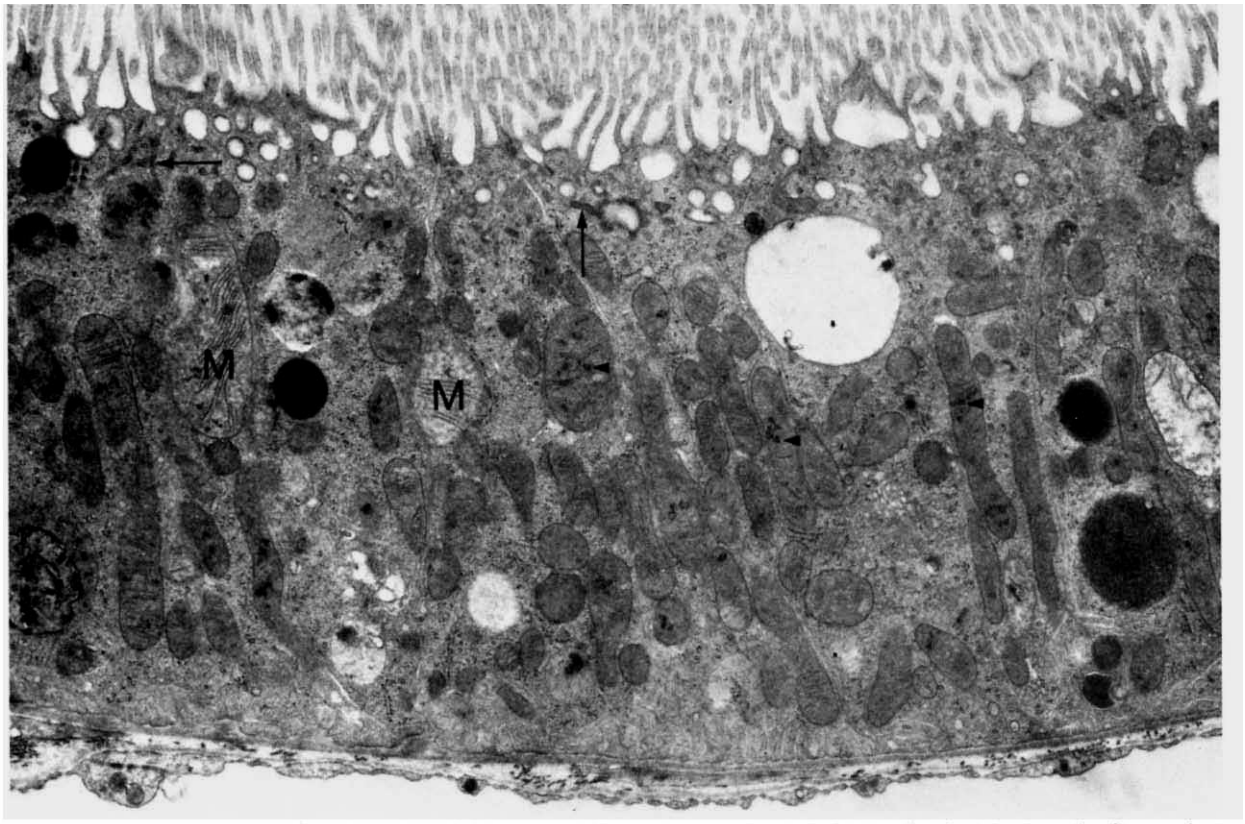

Fig. 8. *Electron micrograph of proximal tubule cells from rat fixed by vascular perfusion 24 hours after the injection of sodium maleate.* The cells appear ultrastructurally normal except that a few mitochondria are dilated (M) and some contain intramitochondrial granules (*arrowheads*), which are more prominent than they are in controls. The apical tubules have reappeared (*arrows*). (×10,500)

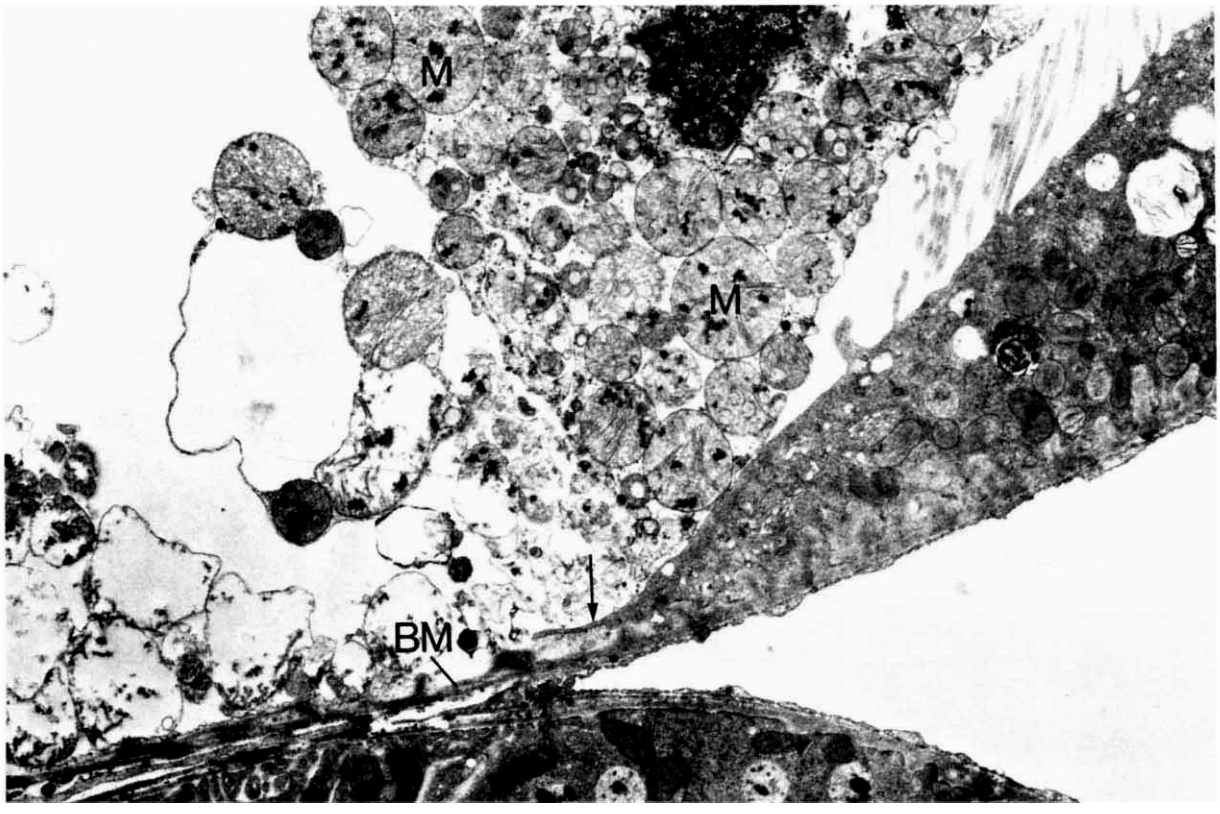

Fig. 9. *Electron micrograph of proximal tubule cells from rat fixed by vascular perfusion 24 hours after injection of sodium maleate.* A necrotic cell, with swollen mitochondria (M) and a pyknotic nucleus (N), seems detached from the basement membrane (BM). Intramitochondrial granules appear increased in size and frequency in many mitochondria. Another cell is extending below the necrotic cell and sends a fingerlike projection along the basement membrane (*arrows*). (×8100)

Table 1. Volume densities (V_V) and volumes per millimeter of tubule length of components of the lysosomal system in proximal tubule cells in sodium-maleate-treated rats and controls[a]

	20 min after 6.0% NaCl	*P*	20 min after sodium maleate	*P*	60 min after sodium maleate	*P*	60 min after 6.0% NaCl
Lysosomes							
V_V, %	6.8 ± 2.7		7.8 ± 1.1	<0.02	12.7 ± 3.4	<0.005	5.1 ± 0.75
Volume, 10^4 μm^3/*mm tubule length*	9.5 ± 2.8		6.8 ± 1.6	<0.05	14.3 ± 6.5		8.0 ± 2.0
Small endocytic vacuoles (<0.5 μm)							
V_V, %	2.3 ± 0.72	<0.02	6.4 ± 2.8	<0.02	10.4 ± 1.0	<0.005	3.0 ± 0.70
Volume, 10^4 μm^3/*mm tubule length*	3.4 ± 1.3		5.8 ± 3.1	<0.02	11.3 ± 2.5	<0.005	4.8 ± 1.7
Large endocytic vacuoles (>0.5 μm)							
V_V, %	2.6 ± 0.19		4.5 ± 1.9		4.7 ± 2.4		4.1 ± 1.1
Volume, 10^4 μm^3/*mm tubule length*	3.9 ± 1.9		3.8 ± 1.7		5.6 ± 3.9		6.6 ± 2.7
All endocytic vacuoles							
V_V, %	4.9 ± 1.8	<0.02	11.0 ± 3.7		15.1 ± 2.7	<0.001	7.0 ± 1.7
Volume, 10^4 μm^3/*mm tubule length*	7.2 ± 3.2		9.6 ± 4.1		16.9 ± 6.3		11.4 ± 4.4
Apical tubules							
V_V, %	1.49 ± 0.75	<0.02	0.26 ± 0.11		0.14 ± 0.08	<0.001	1.62 ± 0.41
Volume, 10^4 μm^3/*mm tubule length*	2.22 ± 1.20	<0.02	0.22 ± 0.05		0.16 ± 0.12	<0.005	2.68 ± 1.16

[a] Values are the means of five animals ± SD. The statistical significance is located between the values being compared.

Table 2. Surface densities (S_V) and surfaces per millimeter of tubule length of microvilli and components of the lysosomal system in sodium-maleate-treated rats and controls[a]

	20 min after 6.0% NaCl	*P*	20 min after sodium maleate	*P*	60 min after sodium maleate	*P*	60 min after 6.0% NaCl
Microvilli							
S_V, $\mu m^2/\mu m^3$	1.3 ± 0.5		2.0 ± 0.8		1.3 ± 0.5		1.7 ± 0.4
Surfaces, 10^6 μm^2/*mm tubule length*	1.9 ± 0.8		1.8 ± 0.9		1.5 ± 0.7		2.7 ± 1.2
Lysosomes							
S_V, $\mu m^2/\mu m^3$	0.35 ± 0.06		0.39 ± 0.06		0.41 ± 0.08		0.29 ± 0.05
Surfaces, 10^6 μm^2/*mm tubule length*	0.50 ± 0.10	<0.05	0.35 ± 0.10		0.46 ± 0.17		0.46 ± 0.15
Small endocytic vacuoles (<0.5 μm)							
S_V, $\mu m^2/\mu m^3$	0.39 ± 0.06	<0.05	1.1 ± 0.6		1.6 ± 0.2	<0.001	0.48 ± 0.06
Surfaces, 10^6 μm^2/*mm tubule length*	0.57 ± 0.12		1.0 ± 0.7		1.8 ± 0.3	<0.001	0.77 ± 0.27
Large endocytic vacuoles (>0.5 μm)							
S_V, $\mu m^2/\mu m^3$	0.17 ± 0.07	<0.05	0.40 ± 0.17		0.38 ± 0.16		0.27 ± 0.08
Surfaces, 10^6 μm^2/*mm tubule length*	0.25 ± 0.12		0.34 ± 0.15		0.44 ± 0.27		0.43 ± 0.18
All endocytic vacuoles							
S_V, $\mu m^2/\mu m^3$	0.56 ± 0.12	<0.02	1.5 ± 0.6		2.0 ± 0.1	<0.001	0.75 ± 0.14
Surfaces, 10^6 μm^2/*mm tubule length*	0.82 ± 0.23		1.3 ± 0.7		2.2 ± 0.5	<0.02	1.2 ± 0.4
Apical tubules							
S_V, $\mu m^2/\mu m^3$	0.60 ± 0.17	<0.005	0.24 ± 0.04	<0.001	0.087 ± 0.036	<0.001	0.61 ± 0.11
Surfaces, 10^6 μm^2/*mm tubule length*	0.89 ± 0.32	<0.005	0.21 ± 0.03	<0.05	0.098 ± 0.054	<0.001	0.96 ± 0.32

[a] Values are the means of five animals ± SD. The statistical significance is located between the values being compared.

transport of absorbed protein into the lysosomes, and lowered the digestion of protein in renal cortical slices. These functional changes occurred simultaneously with significant quantitative alterations of the main components of the vacuolar apparatus, that is, endocytic vacuoles, apical tubules, and lysosomes. In the following, we will correlate the ultrastructural and functional changes and discuss the evidence suggesting that the decreased uptake and digestion of lysozyme is due to a decreased rate of endocytosis and intracellular transport of the tracer protein.

Renal filtration, accumulation, and excretion of lysozyme. The decreased renal accumulation of lysozyme in sodium-maleate-treated rats (9.4%), as compared with controls (39.6%), was partly due to a decrease in GFR and a decrease in the fractional clearance of lysozyme. Because, however, in maleate-treated animals the urinary excretion of lysozyme was 4.4% of the injected and infused dose as compared with 0.2% in controls, it is concluded that the tubular uptake of lysozyme was also decreased by sodium maleate. These results are consistent with the observations of Mogielnicki, Waldman, and Strober [9] and Frederiksson and Petersson [11], who demonstrated that sodium maleate produces a tubular proteinuria. Because our present and previous [13] autoradiographic observations

Table 3. Diameter of lysosomes, cell height, and luminal diameter of proximal tubules in sodium-maleate-treated rats and controls[a]

	20 min after 6.0% NaCl	*P*	20 min after sodium maleate	*P*	60 min after sodium maleate	*P*	60 min after 6.0% NaCl
Diameter of lysosomes, *μm*	1.13 ± 0.28		1.20 ± 0.13	<0.005	1.85 ± 0.28	<0.001	1.06 ± 0.18
Luminal diameter of proximal tubules, *μm*	27.7 ± 2.7	<0.001	38.2 ± 3.0		42.3 ± 4.3	<0.005	31.2 ± 1.4
Height of proximal tubule cells, *μm*	10.9 ± 0.6	<0.001	6.6 ± 1.0		6.9 ± 1.1	<0.02	9.5 ± 1.0

[a] Values are the means of five animals ± SD. The statistical significance is located between the values being compared.

Table 4. Effects of sodium maleate on renal protein accumulation, urinary protein excretion, GFR, and urine flow[a]

	0.9% NaCl	*P*	6.0% NaCl	*P*	Sodium maleate	*P*
Renal lysozyme accumulation, *% of total dose*	29.9 ± 4.7	<0.05	39.6 ± 3.7	<0.001	9.4 ± 2.0	<0.005
Urinary lysozyme excretion, *% of total dose*	0.06 ± 0.01		0.20 ± 0.15	<0.02	4.4 ± 1.7	<0.02
GFR before injections[b], *ml/min*	2.45 ± 0.35		2.70 ± 0.19		3.00 ± 0.61	
GFR after injections[b], *ml/min*	2.66 ± 0.17		2.62 ± 0.08	<0.005	1.57 ± 0.27	<0.005
Clearance lysozyme, *ml/min*	1.52 ± 0.23	<0.05	2.14 ± 0.26	<0.001	0.47 ± 0.12	<0.005
Fractional clearance lysozyme, %	57 ± 5	<0.05	82 ± 11	<0.02	31 ± 12	<0.05
Urine flow before injections[b], *μl urine/min*	1.5 ± 0.4		2.2 ± 1.0		2.5 ± 0.9	
Urine flow after injections[b], *μl urine/min*	3.1 ± 1.5		22 ± 18	<0.005	179 ± 39	<0.005

[a] Values are means of three experiments ± SD. The statistical significance is between the sodium maleate, and the 0.9% NaCl group is given in the column to the right.

[b] For experimental protocol, see methods section.

demonstrated that the lysozyme was absorbed by way of endocytic vacuoles and never accumulated in the cytoplasm, the decreased tubular uptake of lysozyme in sodium-maleate-treated rats is interpreted an effect of a decreased rate of endocytosis.

Endocytosis stimulates ATP synthesis in, for example, polymorphonuclear leukocytes [26] and in fibroblasts agents that decrease the ATP level and also decrease the endocytosis of horseradish peroxidase [27]. Because ATP levels are decreased in kidneys from sodium-maleate-treated rats [5], it is likely that the decreased uptake of lysozyme by means of endocytosis in the present study is due to lack of cellular energy supplies in the form of ATP.

The fractional clearance found for lysozyme in control rats (57%) in the present study is somewhat lower than are the values of 77 to 80% obtained by Maack [28]. It is likely that the latter values are too high because the experiments were performed with isolated perfused rat kidneys where the tubular uptake of protein was inhibited with potassium cyanide or sodium iodoacetate [28]. These substances not only inhibit tubular protein uptake, but also effect glomerular cells and induce glomerular proteinuria. Our value for the fractional clearance of lysozyme, on the other hand, was probably somewhat decreased due to lysosomal digestion because more than 40% of the protein in the proximal tubule cells was located in the lysosomes 15 min (Table 5) after a single injection of labeled lysozyme and thus was exposed to hydrolytic enzymes. This decrease, however, was probably very small because less than 10% of the protein was digested during the first 20 min of incubation (Fig. 14). In comparable experiments with labeled cytochrome C, close to 30% of the tracer was digested during the same conditions [29], indicating that lysozyme and cytochrome C have different susceptibilities to lysosomal catabolism.

The increased renal accumulation of protein in animals receiving 6.0%, as compared with 0.9%, sodium chloride (Table 3) is due to an increased glomerular permeability of lysozyme, as reflected in the fractional clearance for lysozyme, because the GFR was identical in the two groups (Table 4). A decreased GFR, as found in the present study, after injection of 400 mg/kg body wt sodium maleate has previously been observed in mice [9] and in rats [5, 11], whereas 150 to 200 mg of sodium maleate/kg body wt did not cause changes in glomerular functions [9, 11].

Intracellular transport of proteins. The accumulation of endocytic vacuoles in the apical cytoplasm of the proximal tubule cells after sodium maleate injection may have one or more of the following explanations: *(1)* increased rate of formation of vacuoles, *(2)* decreased fusion between vacuoles and lysosomes, or *(3)* modified recycling of membrane

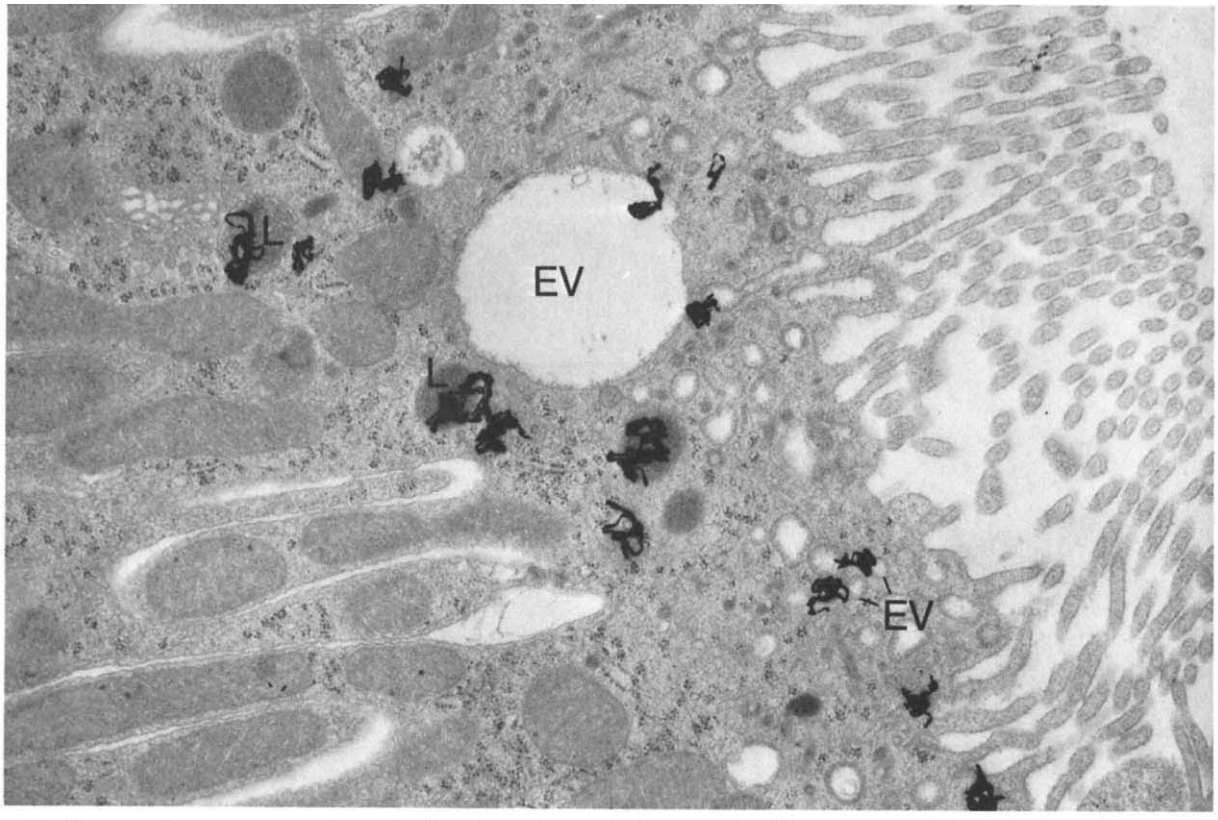

Fig. 10. *Electron microscope autoradiograph of proximal tubule cells from a rat fixed by vascular perfusion 15 min after i.v. injection of labeled lysozyme.* Five minutes before the injection of protein, the rat was injected with 0.9% sodium chloride (control). Most autoradiographic grains are located either over or close to the endocytic vacuoles (EV) or lysosomes (L). (×16,600)

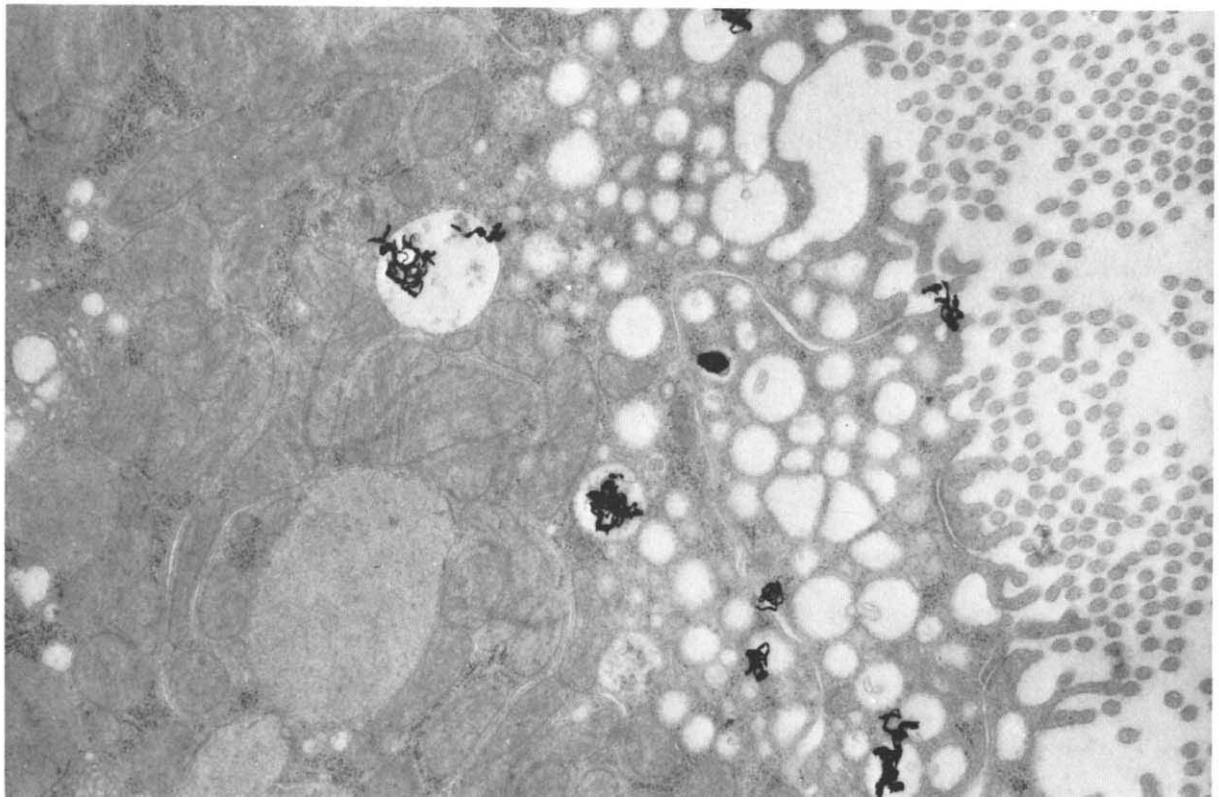

Fig. 11. *Electron microscope autoradiograph of proximal tubule cells from rat prepared as in Fig. 10, but injected with sodium maleate instead of sodium chloride.* Most autoradiographic grains are located directly over the endocytic vacuoles. (×16,600)

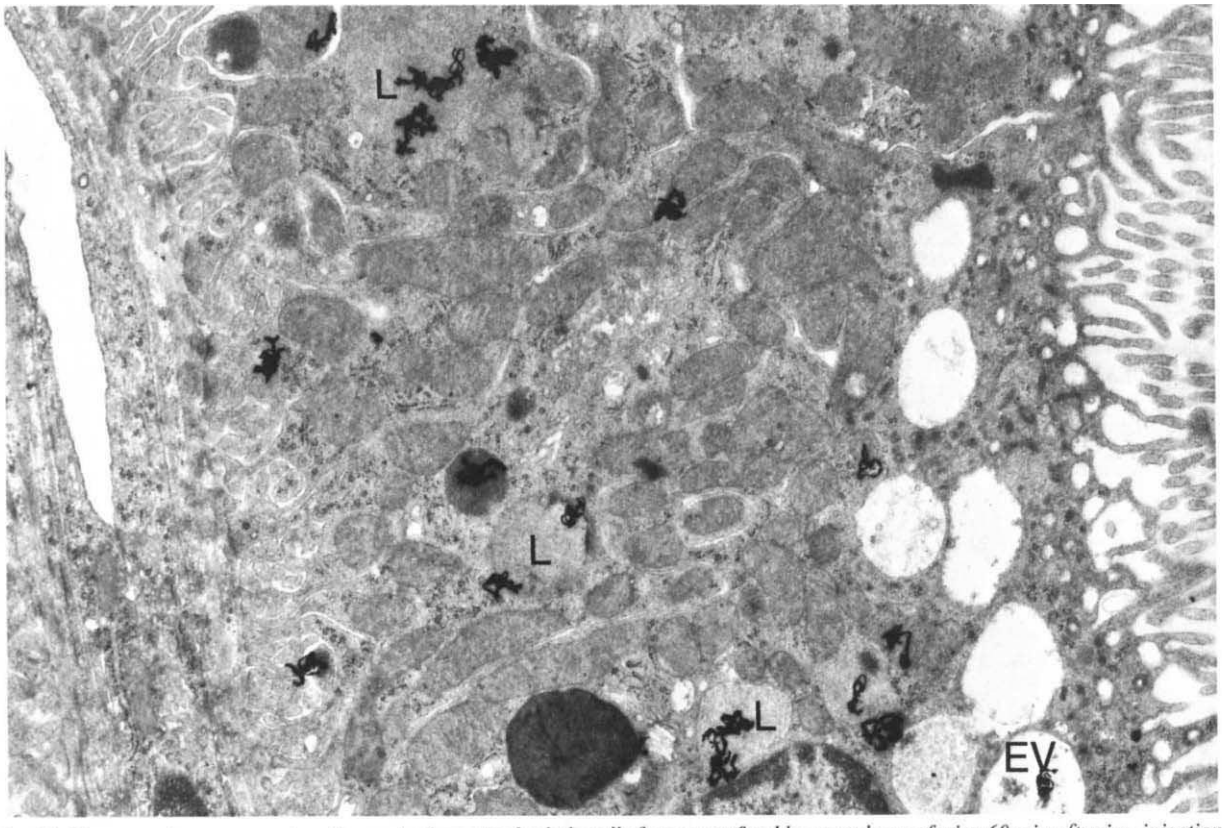

Fig. 12. *Electron microscope autoradiograph of proximal tubule cells from a rat fixed by vascular perfusion 60 min after i.v. injection of labeled lysozyme.* Five minutes before the injection of protein, the rat was injected with 0.9% sodium chloride (control). Most autoradiographic grains are located over lysosomes (L). A single grain can be seen over an endocytic vacuole (EV). (×13,000)

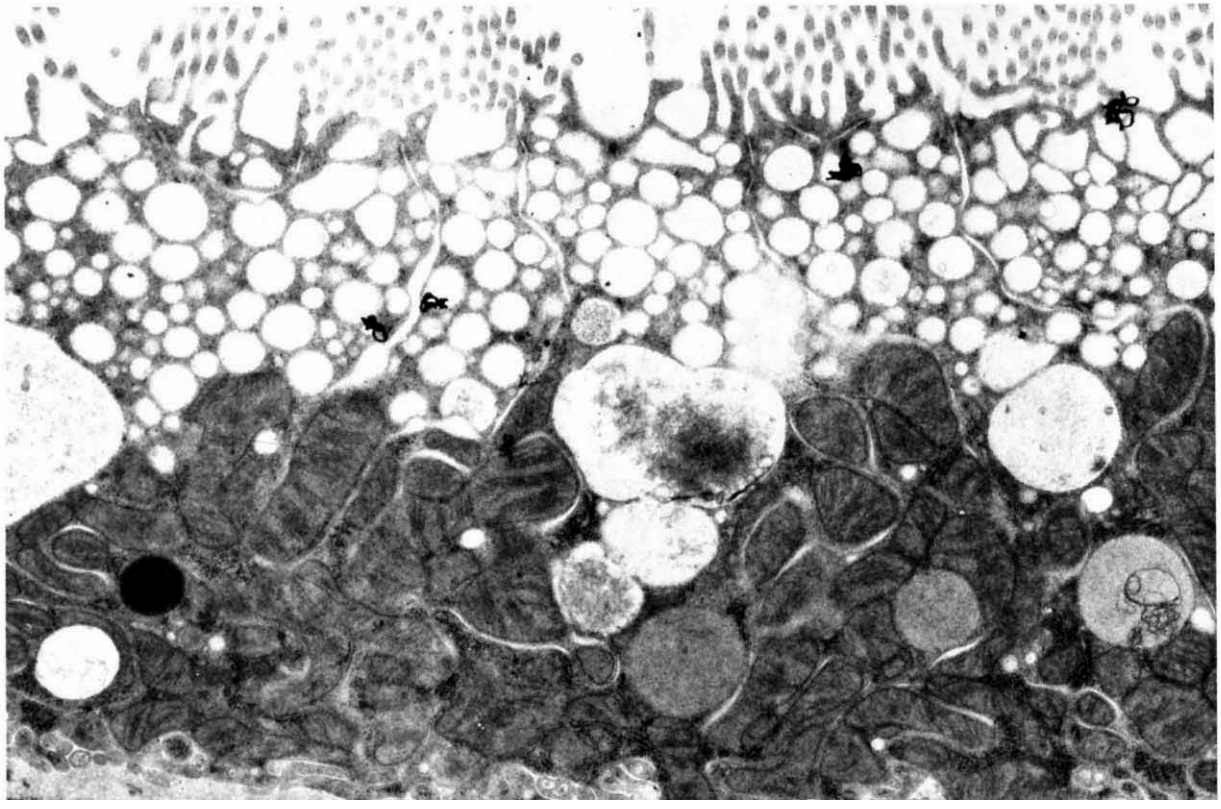

Fig. 13. *Electron microscope autoradiograph of proximal tubule cells from a rat prepared as in Fig. 12, but injected with sodium maleate instead of sodium chloride.* All grains are located over endocytic vacuoles. (×13,000)

Table 5. Distribution of autoradiographic grains over proximal tubule cells following i.v. injection of ^{125}I-lysozyme into rats that were injected 5 min previously with sodium maleate or sodium chloride[a]

Time after injection of lysozyme *min*	Injection	Directly over endocytic vacuoles %	Total endocytic vacuoles[b] %	Directly over lysosomes %	Total lysosomes[c] %	Brush border %	Cytoplasm %	Basement membrane %	Total no. of grains
15	0.9% NaCl	18.0 ± 6.5	43.6 ± 11.7	28.8 ± 8.0	41.6 ± 7.4	4.4 ± 1.0	9.0 ± 3.3	1.4 ± 1.6	881
15	6.0% NaCl	12.7 ± 3.5	34.2 ± 7.5	30.7 ±6.2	47.3 ± 7.1	7.7 ± 4.1	9.1 ± 4.0	1.6 ± 1.4	821
15	Sodium maleate	39.1 ± 7.2	72.3 ± 7.2	4.2 ± 2.9	6.3 ± 4.1	9.4 ± 3.8	8.1 ± 3.2	4.0 ± 2.7	661
60	0.9% NaCl	5.0 ± 2.3	11.5 ± 3.5	61.7 ± 5.6	81.0 ± 6.0	1.0 ± 0.8	5.6 ± 2.6	0.9 ± 0.8	576
60	6.0% NaCl	3.3 ± 1.2	11.9 ± 3.7	53.3 ± 3.8	70.4 ± 6.9	5.8 ± 3.7	11.2 ± 4.4	0.7 ± 1.0	334
60	Sodium maleate	41.4 ± 9.4	80.8 ± 13.9	5.3 ± 5.3	7.5 ± 4.7	2.3 ± 2.8	9.4 ± 14	0	136

[a] The values given as the means ± SD are the percent of total number of grains (N = 4).
[b] The sum of the grains directly over endocytic vacuoles and over the E-cytoplasm (defined in Methods)
[c] The sum of the grains directly over lysosomes and over the L-cytoplasm (defined in Methods)

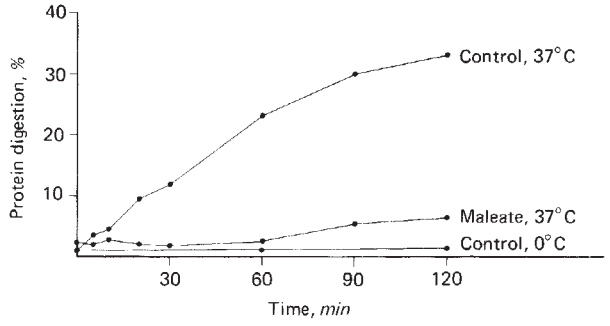

Fig. 14. *Catabolism of ^{125}I-lysozyme in renal cortical slices removed from animals 15 min after i.v. injection of the protein.* Five minutes before injection of the protein the rats were injected with either sodium maleate or 0.9% sodium chloride (control). The incubations were carried out at 37° C or at 0° C. *Ordinate* gives protein catabolism expressed as TCA-soluble radioactivity in incubation medium and slices as percent of total radioactivity. *Abscissa* gives incubation time in minutes. The curves represent the means of two experiments.

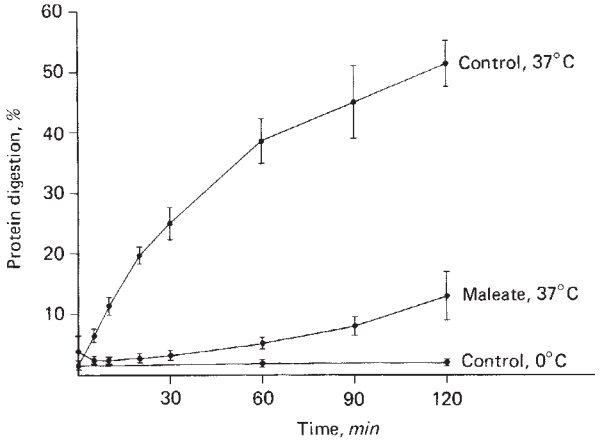

Fig. 15. *Catabolism of ^{125}I-lysozyme in renal cortical slices removed from animals 60 min after i.v. injection of the protein.* Five minutes before injection of the protein, the rats were injected with either sodium maleate or 0.9% sodium chloride (control). Coordinates are the same as they are in Fig. 14 (means ± SD of six experiments).

material between the cell membrane and apical vacuoles or tubules. The first alternative, an increased formation of endocytic vacuoles, seems unlikely because quantitatively the uptake of protein from the tubule lumen was decreased and because maleate probably interferes with the energy production required for endocytosis as discussed above. It is also unlikely that the membrane material added to the endocytic vacuoles was derived from the brush border because there were no significant changes in the surface area of the microvilli of the brush border after injection of sodium maleate (Table 2). The latter observations are consistent with the results of Bode et al [30] suggesting that the brush border membrane and the membranes of the endocytic vacuoles have different chemical compositions and that endocytosis takes place at the luminal plasma membrane at places different from the brush border. The impression that the number of microvilli is reduced in sodium-maleate-treated rats (compare Figs. 1 and 2) is probably due to the increased luminal diameter of the proximal tubule. The surface area of the microvilli found in control rats (1.9 and 2.7 × 10^6 μm^2/mm tubule length) is similar to the value (2.9 × 10^6 μm^2/mm tubule length) found in isolated rabbit proximal tubules [31] and a similar surface area is equivalent to the figure of 40 μm^2 microvilli membrane/μm^2 luminal cell area determined in the first proximal segment of the rat [32].

The possibility that the increased area of membrane in the endocytic vacuoles represents de novo synthesized membrane should also be considered because it has been shown that labeled fucose, which is built into membrane glycoproteins, reached a high concentration in the apical part of the proximal tubule cells by 35 min after i.v. injection following initial incorporation in the Golgi apparatus [33]. Because, however, the accumulation

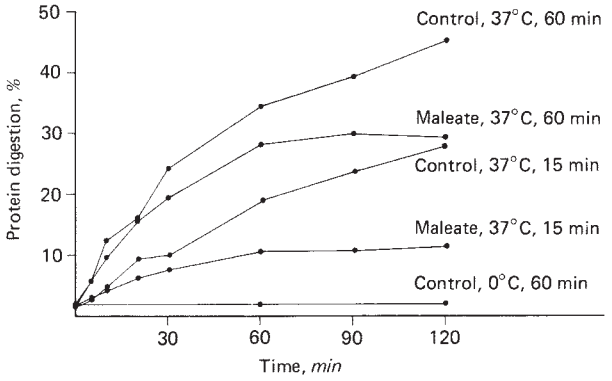

Fig. 16. *Catabolism of ^{125}I-lysozyme in renal cortical slices removed from animals 15 min after i.v. injection of the protein* (curves, labeled 15 min) *or removed 60 min after i.v. injection of the protein* (curves, labeled 60 min). The sodium maleate (2.5 mg/ml) was added to the incubation medium. Coordinates are the same as they are in Fig. 14. The curves represent the means of two experiments.

of endocytic vacuoles appeared even more rapid (Fig. 2), this explanation appears unlikely, in particular because a vesicular transport from the Golgi apparatus may also be decreased after the injection of sodium maleate. It is also unlikely that the vacuoles were derived from primary lysosomes or smooth endoplasmic reticulum, because they lacked acid phosphatase activity (Fig. 6) and because the smooth endoplasmic reticulum appeared unchanged.

The second alternative, that accumulation of endocytic vacuoles is due to a decreased fusion of endocytic vacuoles and lysosomes, is consistent with the autoradiographic demonstration of a tenfold larger amount of protein in the endocytic vacuoles than in the lysosomes after sodium maleate injection, as compared with a sixfold difference in favor of lysosomes in the corresponding controls (Table 5). It is unlikely that the small amount of label in the lysosomes after sodium maleate treatment is caused by digestion of the protein because protein catabolism was greatly reduced after sodium maleate treatment (Fig. 15).

The third possibility, a modified recycling of membrane between the cell membrane and apical vacuoles or tubules, must also be considered as an explanation for the accumulation of endocytic vacuoles. Recycling of membrane has been observed in epithelial cells of the seminal vesicles [34] and secretory cells [35], and it has been suggested by Maunsbach [36], on the basis of protein tracer studies, that one function of the apical tubules is to return membrane material from the endocytic vacuoles to the luminal plasma membrane. It is noteworthy that the surface area of all endocytic vacuoles is not much larger than the surface area of the lysosomes (0.82×10^6 μm^2 vs. 0.50×10^6 μm^2/mm tubule length, Table 2). The endocytic vacuoles, however, have a lifespan of only a few minutes [32, 37] as compared with at least a few weeks for the lysosomes [38]. Therefore, most of the membrane material of the endocytic vacuoles is not incorporated into the lysosomal membranes, but is probably instead recycled from the endocytic vacuoles to the apical cell membrane.

The almost complete disappearance of apical tubules in cells of maleate-treated animals suggests that the tubules either changed into vacuoles or fused with the cell membrane. Both alternatives are consistent with previous observations that demonstrate a close relationship between apical tubules and the apical cell membrane and even direct continuities between apical tubules and apical vacuoles [32, 36]. Our autoradiographic observations indicate that the numerous vacuoles that appear after sodium maleate treatment are endocytic vacuoles that have accumulated due to a decreased rate of fusion with lysosomes. Therefore, the absence of an increase in the combined surface area of apical tubules and vacuoles after maleate (Table 6) does not suggest that the apical vacuoles were formed

Table 6. The combined surface areas or volumes of endocytic vacuoles and apical tubules in proximal tubule cells of sodium maleate treated and control rats[a]

	20 min after 6.0% NaCl	20 min after sodium maleate	*P*	60 min after sodium maleate	*P*	60 min after 6.0% NaCl
Surface area of all endocytic vacuoles and apical tubules, *10^6 μm^2/μm tubule length*	1.7 ± 0.5	1.6 ± 0.8		2.3 ± 0.6		2.2 ± 0.7
Surface area of small endocytic vacuoles and apical tubules, *10^6 μm^2/μm tubule length*	1.5 ± 0.4	1.2 ± 0.8		1.9 ± 0.3		1.7 ± 0.6
Volume of all endocytic vacuoles and apical tubules, *10^4 μm^3/mm tubule length*	9.5 ± 4.3	9.9 ± 4.1		17.1 ± 6.4		14.1 ± 5.5
Volume of small endocytic vacuoles and apical tubules, *10^4 μm^3/mm tubule length*	5.6 ± 2.5	6.0 ± 3.1	<0.02	11.5 ± 2.6	<0.05	7.5 ± 2.8

[a] Values are the means of five animals ± SD. The statistical significance is located between the values being compared.

from apical tubules. Instead, the present observations favor the explanation that the rate of formation of apical tubules from endocytic vacuoles following maleate treatment is lower than the rate of fusion of apical tubules with the cell membrane and indicate that the disappearance of apical tubules is due to membrane transfer from apical tubules to the plasma membrane.

Vesicular transport within protein secreting cells is known to be energy dependent [39]. It appears likely that lack of energy supply is also the cause of the decreased transport of protein from endocytic vacuoles to lysosomes in proximal tubule cells exposed to sodium maleate. Accumulations of apical vesicles, similar to the endocytic vesicles observed after sodium maleate infusion, have also been observed in proximal tubule cells following ischemia [40, 41] and following inhibition of tubular catabolism with potassium cyanide or sodium iodoacetate [42].

Intracellular digestion of protein. The present observations are consistent with our previous demonstration that digestion of protein by proximal tubule cells occurs within the lysosomal system [13]. The decreased digestion of lysozyme in renal cortical slices from sodium-maleate-treated rats probably largely reflects a decreased transport of the protein into the lysosomes as discussed above. This is supported by the observation that sodium maleate added to the incubation medium only partially inhibited lysosomal catabolism in slices (Fig. 16) and, in particular, that the initial inhibitory effect of maleate was small in slices removed 60 min after injection of labeled lysozyme, where most of the tracer was present in the lysosomes already at the start of incubation (Table 5). Furthermore, the possibility that sodium maleate, in addition, has a direct effect on the lysosomal catabolism is also unlikely because we found in preliminary experiments that the digestion of labeled lysozyme by lysosomal enzymes isolated by differential centrifugation from rat renal cortex was not impaired by the addition of sodium maleate to the incubation medium unless very high doses of sodium maleate (5 mg/mg of lysosomal protein, or more) were used.

The observation that the diameter of the lysosomes was larger after sodium maleate treatment for 60 min than it was after 20 min despite the lysosomal surface area per millimeter of tubule length was unchanged suggests that there was a change towards fewer, but larger lysosomes. There was no evidence that the size of the lysosomes was related to the efficiency of digestion because protein digestion was decreased not only in slices removed 1 hour after injection of sodium maleate, but also to a similar degree in slices removed after 15 min when there were no changes in the lysosomal diameter. This conclusion is in agreement with previous observations, that protein catabolism was not decreased in dextran-absorbing kidney cells despite considerable increases in the dimensions of the lysosomes [43].

Acknowledgments

This work was presented in part at the Annual Meeting of the Scandinavian Society for Electron Microscopy in Uppsala, Sweden, June 6–7, 1977 [44]. The investigation was supported from the University of Aarhus and in part by the Danish Medical Research Council. Mrs. M. A. Jensen, Mrs. B. Overgaard, and Mr. P. Boldsen provided technical assistance, and Miss K. Svendsen typed the manuscript.

Reprint requests to Dr. A. B. Maunsbach, Department of Cell Biology, Institute of Anatomy, University of Aarhus, DK-8000 Aarhus C, Denmark

References

1. Berliner RW, Kennedy TJ, Hilton JG: Effect of maleic acid on renal function. *Proc Soc Exp Biol Med* 75:791–794, 1950
2. Harrison HE, Harrison HC: Experimental production of renal glycosuria, phosphaturia, and aminoaciduria by injection of maleic acid. *Science* 120:606–608, 1954
3. Angielski S, Rogulski J, Mikulski P, Popinigis J: Aminoaciduria induced with maleic acid. IV. Amino nitrogen and ketoacids in blood. *Acta Biochim Pol* 8:285–293, 1960
4. Rogulski J, Pacanis A, Adamowicz W, Angielski S: On the mechanism of maleate action on rat kidney mitochondria: Effect on oxidative metabolism. *Acta Biochim Pol* 21:403–413, 1974
5. Kramer HJ, Gonick HC: Experimental Fanconi syndrome: I. Effect of maleic acid on renal cortical Na,K-ATPase activity and ATP levels. *J Lab Clin Med* 76:799–808, 1970
6. Worthen HG: Renal toxicity of maleic acid in the rat: Enzymatic and morphologic observations. *Lab Invest* 12:791–801, 1963
7. Schärer K, Yoshida T, Voyer L, Berlow S, Pietra G, Metcoff J: Impaired renal gluconeogenesis and energy metabolism in maleic acid-induced nephropathy in rats. *Res Exp Med* 157:136–152, 1972
8. Rosen VJ, Kramer HJ, Gonick HC: Experimental Fanconi syndrome: II. Effect of maleic acid on renal tubular ultrastructure. *Lab Invest* 28:446–455, 1973
9. Mogielnicki RP, Waldman TA, Strober W: Renal handling of low molecular weight proteins: I. L-chain metabolism in experimental renal disease. *J Clin Invest* 50:901–909, 1971
10. Kramer HJ, Gonick HC: Effect of maleic acid on sodium-

linked tubular transport in experimental Fanconi syndrome. *Nephron* 10:306–319, 1973

11. FREDERIKSSON Å, PETERSON PA: Effects of renal dysfunction on β_2-microglobulin metabolism. *Scand J Urol Nephrol* 26(Suppl):61–76, 1975
12. FUJITA T, ITAKURA M: Renal handling of lysozyme in experimental Fanconi syndrome. *J Lab Clin Med* 92:135–140, 1978
13. CHRISTENSEN EI, MAUNSBACH AB: Intralysosomal digestion of lysozyme in renal proximal tubule cells. *Kidney Int* 6:396–407, 1974
14. MCFARLANE AS: Efficient trace-labelling of proteins with iodine. *Nature* 182:53, 1958
15. IZZO JL, BALE WF, IZZO MJ, RONCONE A: High specific activity labeling of insulin with ^{131}I. *J Biol Chem* 239:3743–3748, 1964
16. LITWACK G: Photometric determination of lysozyme activity. *Proc Soc Exp Biol Med* 89:401–403, 1955
17. LOWRY OH, ROSEBROUGH NJ, FARR AL, RANDALL RJ: Protein measurement with the Folin phenol reagent. *J Biol Chem* 193:265–275, 1951
18. MAUDE DL: Stop-flow microperfusion of proximal tubules in rat kidney cortex slices. *Am J Physiol* 214:1315–1321, 1968
19. MAUNSBACH AB: The influence of different fixatives and fixation methods on the ultrastructure of rat kidney proximal tubule cells: I. Comparison of different perfusion fixation methods and of glutaraldehyde, formaldehyde and osmium tetroxide fixatives. *J Ultrastruct Res* 15:242–282, 1966
20. WEIBEL ER, KISTLER GS, SCHERLE WF: Practical stereological methods for morphometric cytology. *J Cell Biol* 30:23–28, 1966
21. GUNDERSEN HJG: Estimation of tubule or cylinder L_v, S_v and V_v on thick sections. *J Microsc*, 117:353–345, 1979
22. GUNDERSEN HJG: Notes on the estimation of the numerical density of arbitrary profiles: the edge effect. *J Microsc* 111:219–223, 1977
23. WEIBEL ER: Stereological principles for morphometry in electron microscopic cytology, in *International Review of Cytology*, edited by BOURNE GH, DANIELLI JF, New York and London, Academic Press, 1969, vol. 26, p. 235
24. BARKA T, ANDERSON J: Histochemical methods for acid phosphatase using hexazonium pararosanilin as coupler. *J Histochem Cytochem* 10:741–753, 1962
25. MAUNSBACH AB: Absorption of I^{125}-labeled homologous albumin by rat kidney proximal tubule cells. A study of microperfused single proximal tubules by electron microscopic autoradiography and histochemistry. *J Ultrastruct Res* 15:197–241, 1966
26. KARNOVSKY ML: Metabolic basis of phagocytic activity. *Physiol Rev* 42:143–168, 1962
27. STEINMAN RM, SILVER JM, COHN ZA: Pinocytosis in fibroblasts: Quantitative studies in vitro. *J Cell Biol* 63:949–969, 1974
28. MAACK T: Renal handling of low molecular weight proteins. *Am J Med* 58:57–64, 1975
29. CHRISTENSEN EI: Rapid protein uptake and digestion in proximal tubule lysosomes. *Kidney Int* 10:301–310, 1976
30. BODE F, POCKRANDT-HEMSTEDT H, BAUMANN K, KINNE R: Analysis of the pinocytic process in rat kidney: I. Isolation of pinocytic vesicles from rat kidney cortex. *J Cell Biol* 63:998–1008, 1974
31. WELLING LW, WELLING DJ: Surface areas of brush border and lateral cell walls in the rabbit proximal nephron. *Kidney Int* 8:343–348, 1975
32. MAUNSBACH AB: Ultrastructure of the proximal tubule, in *Handbook of Physiology, Section 8: Renal Physiology*, edited by ORLOFF J, BERLINER RW, Washington D.C., American Physiological Society, 1973, p. 31
33. HADDAD A, BENNETT G, LEBLOND CP: Formation and turnover of plasma membrane glycoproteins in kidney tubules of young rats and adult mice, as shown by autoradiography after an injection of ^{3}H-fucose. *Am J Physiol* 148:241–274, 1977
34. MATA LR, DAVID-FERREIRA JF: Transport of exogenous peroxidase to Golgi cisternae in the hamster seminal vesicle. *J Microscopie* 17:103–106, 1973
35. HERZOG V, FARQUHAR MG: Luminal membrane retrieved after exocytosis reaches most Golgi cisternae in secretory cells. *Proc Natl Acad Sci USA* 74:5073–5077, 1977
36. MAUNSBACH AB: Cellular mechanisms of tubular protein transport, Chapter 5, in *International Review of Physiology, Kidney and Urinary Physiology II*, edited by THURAU K, Baltimore, University Park Press, 1976, vol. 11, p. 145
37. MAUNSBACH AB: Absorption of ferritin by rat kidney proximal tubule cells: Electron microscopic observations of the initial uptake phase in cells of microperfused single proximal tubules. *J Ultrastruct Res* 16:1–12, 1966
38. DINGLE JT, BARRETT AJ: Uptake of biologically active substances by lysosomes. *Proc R Soc London [B]* 173:85–93, 1969
39. JAMIESON JD, PALADE GE: Intracellular transport of secretory proteins in the pancreatic exocrine cell: IV. Metabolic requirements. *J Cell Biol* 39:589–603, 1968
40. REIMER KA, GANOTE CE, JENNINGS RB: Alterations in renal cortex following ischemic injury: III. Ultrastructure of proximal tubules after ischemia or autolysis. *Lab Invest* 26:347–363, 1972
41. DONOHOE JF, VENKATACHALAM MA, BERNARD DB, LEVINSKY NG: Tubular leakage and obstruction after renal ischemia: Structural-functional correlations. *Kidney Int* 13:208–222, 1978
42. LANGER KH, THOENES W: Zur Genese "optisch leerer Vakuolen" im Epithel des energetisch insuffizienten proximalen Nierentubulus: Untersuchungen an der Rattenniere nach Kaliumcyanidvergiftung und hämorrhagischem Schock. *Verh Dtsch Ges Pathol* 53:394–400, 1969
43. CHRISTENSEN EI, MAUNSBACH AB: Effects of dextran on lysosomal ultrastructure and protein digestion in renal proximal tubule. *Kidney Int*, 16:301–311, 1979
44. CHRISTENSEN EI, MAUNSBACH AB: Effects of sodium maleate on endocytosis and lysosomal protein catabolism in proximal tubule cells. *J Ultrastruct Res* 63:91–92, 1978